Article

Detaching Thiolates from Copper and Gold Clusters: Which Bonds to Break?

Martin Konpka, Roger Rousseau, Ivan tich, and Dominik Marx

J. Am. Chem. Soc., **2004**, 126 (38), 12103-12111• DOI: 10.1021/ja047946j • Publication Date (Web): 04 September 2004

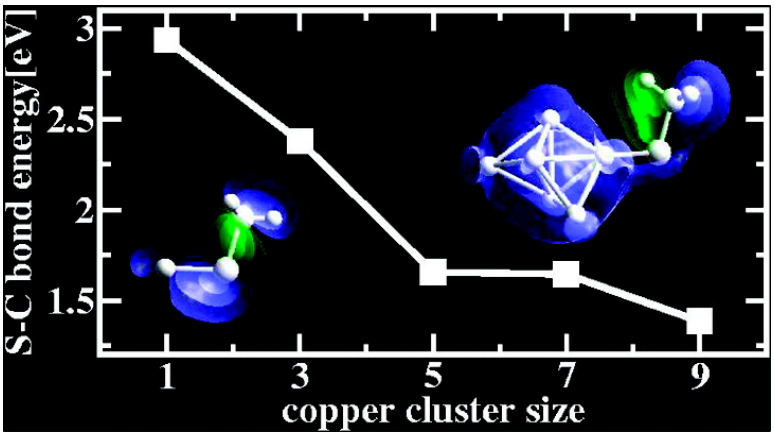

More About This Article

Additional resources and features associated with this article are available within the HTML version:

- Supporting Information
- Links to the 8 articles that cite this article, as of the time of this article download
- Access to high resolution figures
- Links to articles and content related to this article
- Copyright permission to reproduce figures and/or text from this article

View the Full Text HTML

J|A|C|S
ARTICLES
Published on Web 09/04/2004

Detaching Thiolates from Copper and Gold Clusters: Which Bonds to Break?

Martin Konôpka,*,† Roger Rousseau,‡ Ivan Štich,† and Dominik Marx§

Contribution from the Center for Computational Materials Science (CCMS), Slovak University of Technology (FEI STU), Ilkovičova 3, 81219, Bratislava, Slovakia; International School for Advanced Studies (ISAS/SISSA), 4 Via Beirut, 34014 Trieste, Italy; and Lehrstuhl für Theoretische Chemie, Ruhr-Universität Bochum, 44780 Bochum, Germany

Received April 9, 2004; E-mail: martin.konopka@stuba.sk

Abstract: The interaction of alkanethiolates with small coinage metal clusters of copper and gold was studied based on density functional theory with a focus on the metal−thiolate junction. Calculation of fragmentation energies indicate that for Cu_n−thiolate ($n = 1,3,5,7$, and 9) there is a progressive lowering in energy for the fragmentation of the S−C bond in the thiolate from a value of 2.9 eV for $n = 1$ to 1.4 eV for $n = 9$. The detailed electronic origins of this specific weakening are attributed to a polarization of electron density in the S−C bond as induced by bonding with the Cu_n cluster. For the gold analogues, this effect is not observed and fragmentation at the S−C bond experiences only a slight 10% destabilization as n increases from 3 to 9. The relativistic origin of this difference between Cu and Au is discussed, and an analysis of bonding considerations is presented.

1. Introduction

Self-assembled monolayers (SAMs) of organic molecules on coinage metal surfaces are currently among the most studied surface systems[1−4] with a number of potential applications ranging from surface coating and lubrication[5] to molecular electronics.[6] Of these, the most studied SAM system is thiolates on gold surfaces.[2] Relative ease of its preparation and its unusually high degree of order make this system a prototypical SAM. In distinct contrast to gold, comparatively little work has been done on thiolate bonding to other coinage metals. Here, copper is especially interesting as a much cheaper potential substitute for gold. However, available experimental evidence suggests that substitution of Au by Cu also modifies the underlying chemistry at the metal−molecule junction. Hence, the thiolate−Cu bond needs to be analyzed and understood.

There are several experimental studies confirming thiolate SAMs formation on low-index Cu surfaces. X-ray standing waves and STM studies of adsorption of short-chain alkylthiolates on Cu(111)[7−9] suggest the existence of a thiolate phase at low temperature and coexistence of different low- and high-temperature thiolate phases, but also an atomic sulfur phase at room temperature. Similarly, highly ordered thiolate phases and, at higher temperatures, atomic S phases or combinations of the above were observed on Cu(100) and Cu(110) surfaces using thermal desorption and XPS techniques.[10,11] Experiments also suggest a *completely different thermal dissociation* of thiolates on Au and Cu surfaces. Heating the Cu(111) surface covered by a $S-CH_3$ adlayer desorbs CH_3 radicals,[7] whereas molecular $S-CH_3$ desorbs from the Au(111) counterpart.[12] Conversely, it has recently been reported that thiolates may be desorbed electrochemically from Cu, Ag, and Au.[13] In this context, sulfur bonded to metal surfaces or clusters is an important topic in copper colloids and biosensors, as well as in catalysis,[14] where mechanisms of desulfurization and catalyst poisoning by sulfur are major issues.

Considering detaching molecules from surfaces, we note that various different mechanisms are conceivable. The obvious one is the thermal desorption mentioned above. An alternate approach is provided by "mechanochemistry"[15] where mechanical energy, instead of thermal energy that is traditionally employed, is used to induce chemical reactions. Given the importance of atomic force microscopy (AFM) and other mechanical techniques in the study of SAMs, it is important to

† Slovak University of Technology (FEI STU).
‡ International School for Advanced Studies (ISAS/SISSA).
§ Ruhr-Universität Bochum.

(1) Ulman, A. *An Introduction to Ultrathin Organic Films: From Langmuir−Blodgett to Self-Assembly*; Academic: San Diego, CA, 1991.
(2) Yang, G.; Liu, G.-y. *J. Phys. Chem. B* **2003**, *107*, 8746−8759.
(3) Ulman, A. *Chem. Rev.* **1996**, *96*, 1533−1554.
(4) Lavrich, D. J.; Wetterer, S. M.; Bernasek, S. L.; Scoles, G. *J. Phys. Chem. B* **1998**, *102*, 3456−3465.
(5) Bhushan, B. *Principles and Applications of Tribology*; Wiley: New York, 1999.
(6) (a) Reichert, J.; Ochs, R.; Beckmann, D.; Weber, H. B.; Mayor, M.; von Löhneysen, H. *Phys. Rev. Lett.* **2002**, *88*, 176804−1−4. (b) Zhou, C.; Deshpande, M. R.; Reed, M. A.; Jones, L., II; Tour, J. M. *Appl. Phys. Lett.* **1997**, *71*, 611−613.
(7) Jackson, G. J.; Woodruff, D. P.; Jones, R. G.; Singh, N. K.; Chan, A. S. Y.; Cowie, B. C. C.; Formoso, V. *Phys. Rev. Lett.* **2000**, *84*, 119−122.
(8) Driver, S. M.; Woodruff, D. P. *Surf. Sci.* **2000**, *457*, 11−23.
(9) Driver, S. M.; Woodruff, D. P. *Surf. Sci.* **2001**, *479*, 1−10.
(10) Vollmer, S.; Witte, G.; Wöll, Ch. *Langmuir* **2001**, *17*, 7560−7565.
(11) Lai, Y.-H.; Yeh, C.-T.; Cheng, S.-H.; Liao, P.; Hung, W.-H. *J. Phys. Chem. B* **2002**, *106*, 5438−5446.
(12) Kondoh, H.; Kodama, C.; Sumida, H.; Nozoye, H. *J. Chem. Phys.* **1999**, *111*, 1175−1184.
(13) Azzaroni, O.; Vela, M. E.; Fonticelli, M.; Benítez, G.; Carro, P.; Blum, B.; Salvarezza, R. C. *J. Phys. Chem. B* **2003**, *107*, 13446−13454.
(14) Rodriguez, J. A.; Hrbek, J. *Acc. Chem. Res.* **1999**, *32*, 719−728.
(15) Krüger, D.; Rousseau, R.; Fuchs, H.; Marx, D. *Angew. Chem.* **2003**, *115*, 2353−2355; *Angew. Chem., Int. Ed.* **2003**, *42*, 2251−2253.

know low energy fragmentation patterns of thiols adsorbed onto various metal species. Such a proposition was studied experimentally[16] and in recent simulations, where the pulling-induced rupture process was investigated for thiolate−gold contacts.[15,17] These simulations strongly indicated that, instead of detaching a thiolate radical with the associated breaking of the Au−S contact, a series of complex isomerization steps involving Au atoms led to the formation of monatomic gold nanowires. Hence, different bond scission scenarios can be obtained by using mechanical and thermal energy.

Given that the thiolate−Au SAM is of great technological importance, there now exists a vast body of theoretical work devoted to this ubiquitous organo−metallic interface. Still, even for this well studied system the theoretical description which would provide a detailed chemical understanding of the Au−S bond itself only starts emerging. Recent theoretical studies of short alkanethiolates on a Au(111) surface[18−21] suggest a strongly covalent Au−S bond with a bridge site as ground-state structure for methylthiolate. However, it is of great interest to compare those results to other related systems such as *clusters* deposited or grown on substrates[22] or surfaces. Small thiolated Au clusters have been recently studied[23] using density functional theory (DFT) techniques. The main finding was the presence of a very strongly covalent, distinctly directional Au−S−C bond and (on the basis of fragmentation energies) preference of dissociation into smaller Au and Au−thiolate clusters, as opposed to breaking the Au−S bond and detaching the Au cluster from the thiolate radical.

In contrast, to the best of our knowledge, only two theoretical DFT studies of Cu−thiolate SAMs exists.[13,19] Both investigations consider a simplified model of methylthiolate radical adsorption on (111) surfaces of Au, Ag, and Cu as modeled by a small two-layer thick closest-packed cluster. In one of these works[19] adsorption energies of neutral methylthiolates were found decreasing in the order Cu>Ag>Au, consistent with experimental findings.[10,12,13] Based on Mulliken population analysis, the Cu−S bond was proposed strongly covalent and relativistic effects were found responsible for covalent features in the Au−S bond, while the Ag−S one was found essentially ionic.[19] The strongly covalent Cu−S bond looks counterintuitive for the essentially nonrelativistic copper. We discuss in detail these issues; vide infra.

In this context we mention that significant relativistic effects[24−26] which exist in Au are absent from other coinage metals. However, the consequences of this well-known fact for chemical bonds relevant to thermal- and mechanochemistry, in particular the thiolate−metal and S−C bonds, are very hard to predict a priori.[19] Relativistic effects strongly contract the s shell-(s) leading to a preference for low coordination/low dimensionality;[27,28] for a careful general discussion of the origin of "relativistic contractions", we refer to ref 24 (Sect.II.D therein). These phenomena manifest themselves by unusual surface reconstructions of low-index Au surfaces, a preference to form planar cluster structures,[29−32] and a tendency to form wires when pulled using mechanically controllable break junctions[28,33] or a "thiolate hook".[17] Another important relativistic implication affecting the Au−S thiolate bond pointed out in ref 19 is a weakening of the Au−S bond on the surface due to simultaneous relativistic contraction of the 6s orbital and stabilization of the $6p_z$ orbital with increasing size of the Au substrate.

Hence, very interesting behavior may be expected as a function of *system dimensionality* and type of the *coinage metal*. It is our aim to investigate structure, energetics, dissociation pathways, and bonding of thiolates chemisorbed onto small Cu_n and Au_n clusters as a function of n as well as corresponding bulk surface limits for reference. We provide a detailed analysis of the evolution of S−C versus M−S bonds for M = Cu and Au as a function of system size with a particular focus on the effects of relativity on the S−C bond.

2. Models and Methods

2.1. Structural Models. The present study targets at investigating systematically neutral $CH_3-(CH_2)_m-S-M_n$ adducts (where $m = 0$, 1 and $n = 1$, 3, 5, 7, 9, the metal atom M being Cu and Au) and their neutral, cationic, and anionic dissociation fragments in order to assess different reaction channels. For the sake of comparison, relevant results from a related study of the Cu(111) and Au(111) surfaces are also included;[34] see also Supporting Information (SI). We only consider these surface results as "asymptotic" ($n \rightarrow \infty$) reference values for fragmentation energies. We limit the cluster sizes M_n to odd numbers n as to avoid further complications due to unpaired electrons and open shells in thiolate−M adducts. One reason for considering n only up to 9 is that the atomistic structures of the Cu_n clusters have been studied previously only up to $n = 10$[35,36] and searching for low-energy $n > 10$ isomers represents a complicated task in its own right. Hence, starting structures for Cu_n were employed from previous work, but all hydrocarbon species, M_n, M_nS, and thiolate−M_n were fully optimized to their nearest local minimum on their respective potential energy surfaces. To facilitate comparison with copper, the gold cluster structures which we employ here are, except the $n = 3$ adduct, isostructural with those used for copper, although they are at most higher in energy by about 0.1 eV than other isomers.

(16) Grandbois, M.; Beyer, M.; Rief, M.; Clausen-Schaumann, H.; Gaub, H. E. *Science* **1999**, *283*, 1727−1730.
(17) Krüger, D.; Fuchs, H.; Rousseau, R.; Marx, D.; Parrinello, M. *Phys. Rev. Lett.* **2002**, *89*, 186402−1−4.
(18) (a) Yourdshahyan, Y.; Zhang, H. K.; Rappe, A. M. *Phys. Rev. B* **2001**, *63*, 081405−1−4(R). (b) Yourdshahyan, Y.; Rappe, A. M. *J. Chem. Phys.* **2002**, *117*, 825−833.
(19) Akinaga, Y.; Nakajima, T.; Hirao, K. *J. Chem. Phys.* **2001**, *114*, 8555−8564.
(20) Tachibana, M.; Yoshizawa, K.; Ogawa, A.; Fujimoto, H.; Hoffmann, R. *J. Phys. Chem. B* **2002**, *106*, 12727−12736.
(21) Vargas, M. C.; Giannozzi, P.; Selloni, A.; Scoles, G. *J. Phys. Chem. B* **2001**, *105*, 9509−9513.
(22) For instance, see: (a) *Metal Clusters at Surfaces*; Meiwes-Broer, K.-H., Ed.; Springer: Berlin, 2000. (b) Daniel, M.-Ch.; Astruc, D. *Chem. Rev.* **2004**, *104*, 293−346.
(23) Krüger, D.; Fuchs, H.; Rousseau, R.; Marx, D.; Parrinello, M. *J. Chem. Phys.* **2001**, *115*, 4776−4786.
(24) Pyykkö, P. *Chem. Rev.* **1988**, *88*, 563−594.
(25) Takeuchi, N.; Chan, C. T.; Ho, K. M. *Phys. Rev. Lett.* **1989**, *63*, 1273−1276; *Phys. Rev. B* **1991**, *43*, 14363−14370.
(26) Pyykkö, P. *Angew. Chem., Int. Ed.* **2002**, *41*, 3573−3578; Theoretical Chemistry of Gold ("Review"). *Angew. Chem., Int. Ed.*, in press.
(27) Bahn, S. R.; Jacobsen, K. W. *Phys. Rev. Lett.* **2001**, *87*, 266101-1-4.
(28) Smit, R. H. M.; Untiedt, C.; Yanson, A. I.; van Ruitenbeek, J. M. *Phys. Rev. Lett.* **2001**, *87*, 266102-1-4.
(29) Rousseau, R.; Dietrich, G.; Krückeberg, S.; Lützenkirchen, K.; Marx, D.; Schweikhard, L.; Walther, C. *Chem. Phys. Lett.* **1998**, *295*, 41−46. See also ref 30.
(30) (a) Rousseau, R.; Marx, D. *J. Chem. Phys.* **2000**, *112*, 761−769. (b) Dietrich, G.; Krückeberg, S.; Lützenkirchen, K.; Schweikhard, L.; Walther, C. *J. Chem. Phys.* **2000**, *112*, 752−760.
(31) Häkkinen, H.; Moseler, M.; Landman, U. *Phys. Rev. Lett.* **2002**, *89*, 033401-1-4.
(32) Furche, F.; Ahlrichs, R.; Weis, P.; Jacob, Ch.; Gilb, S.; Bierweiler, T.; Kappes, M. M. *J. Chem. Phys.* **2002**, *117*, 6982−6990.
(33) Rubio-Bollinger, G.; Bahn, S. R.; Agraït, N.; Jacobsen, K. W.; Vieira, S. *Phys. Rev. Lett.* **2001**, *87*, 026101-1-4.
(34) Konôpka, M.; Rousseau, R.; Štich, I.; Marx, D. In preparation.
(35) Jug, K.; Zimmermann, B.; Calaminici, P.; Köster, A. M. *J. Chem. Phys.* **2002**, *116*, 4497−4507. We noticed that cancellation of errors from local density approximation and insufficient basis set led to relatively accurate structures in this work.
(36) Jaque, P.; Toro-Labbé, A. *J. Chem. Phys.* **2002**, *117*, 3208−3218.

In experimental studies, various thiolate chain lengths are used, from $n = 1^{7-9}$ up to, e.g., $n = 30$.[37] A computational study based on these systems would be more expensive employing a fully ab initio description of the alkyl chain and is more appropriate for mixed quantum/classical mechanics hybrid methods.[38,39] However, our previous study of thiolated Au clusters[23] as well as a related surface study[40] demonstrated that adsorption and fragmentation energies obtained with chains as short as two (one) carbon atoms provide accurate quantitative (qualitative) representatives for results with longer chains. For those reasons, we have considered thiolate species with up to two carbon atoms only.

2.2. Electronic Structure Methods and Optimization Techniques. The majority of our results were obtained in the framework of the DFT[41] with the (spin polarized) PBE functional[42] and plane-wave basis sets using the CPMD software package.[43] Several calculations, in particular Mulliken populations analysis, were performed using the CASTEP[44] plane-wave code (relying on identical sets of pseudopotentials). Using the same plane-wave approach for thiolates on surfaces (slab models with periodic boundary conditions in this case) allows for consistent comparisons between data obtained for clusters and extended systems. For all cluster calculations with CPMD, we employed nonperiodic boundary conditions.[45]

The calculations involving Cu were performed with PBE ultrasoft pseudopotentials[46,47] throughout with a plane-wave cutoff of 25 Ry, including the 3d and 4s valence electrons of scalar-relativistic Cu. This "large core" 11-electron Cu pseudopotential was tested against the potentially more accurate "small core" ultrasoft pseudopotential with 19 electrons in the valence subspace with only a small difference in results; see SI. Only the calculations involving Au clusters were performed with an analogous prescription as used previously in ref 23, i.e., an 11-electron scalar-relativistic norm-conserving PBE pseudopotential for Au and a cutoff of 60 Ry. All CPMD calculations were done in a large supercell with an edge length of 13 Å for Cu and 14 Å for Au. This plane-wave DFT (PBE) approach, either using CPMD or CASTEP, is abbreviated by "pwPBE".

For the sake of comparison we have also performed extensive calculations using the GAUSSIAN98 package[48] with the PBE functional and second-order Møller−Plesset perturbation theory (MP2). This allows us to assess the pseudopotential approximation and the importance of van der Waals interactions. Results of these extensive accuracy tests are shown in SI. In brief, the de facto limitations of both Gaussian and plane-wave approaches for the system sizes of interest place limitations on our results on the order of a few tenths of an eV. Most importantly, however, both methods preserve the same qualitative picture, namely fragmentation into neutral products, and homolytic S−C bond cleavage and thiolate radical desorption as energetically competitive processes at all levels of theory, including MP2. The relative error induced by Gaussian basis set size was found more significant than that resulting from use of the pseudopotential approximation. Therefore, the results we present here are those obtained with the pwPBE method.

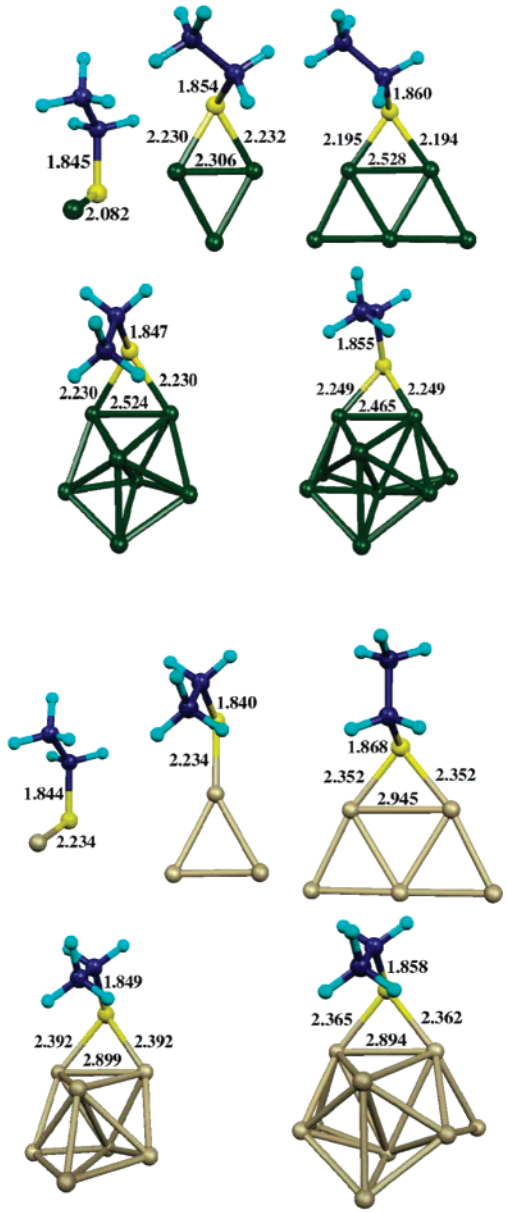

Figure 1. Relaxed geometries of the $CH_3-CH_2-S-Cu_n$ (upper panel) and $CH_3-CH_2-S-Au_n$ (lower panel) adducts for $n = 1$, 3, 5, 7, and 9. Interatomic distances are given in Å, and MOLEKEL visualization software[49] was used.

We allowed for full relaxation of all coordinates of all adducts and their fragments considered in the present work. Symmetry unrestricted structural relaxations were performed using local-optimization methods implemented in CPMD and GAUSSIAN98. These approaches do not necessarily lead to the global minimum for cluster adducts of the given size; nonetheless, they will provide stable low energy minima which are best viewed as "representative structures"[23] which is all that is required for the current study. We note that the resulting Au_n clusters are isostructural with well-known low energy species in all cases including $n = 7$ and 9; see refs 29 and 30. All methylthiolate−Cu_n ($n = 1$, 3, 5, 7, and 9) species are isostructural to their ethyl-analogues as illustrated in Figure 1. Investigation of reaction coordinates for some of the fragmentation scenarios reported here were performed using the QST2 and QST3 methods.[48]

(37) Jennings, G. K.; Munro, J. C.; Yong, T.-H.; Laibinis, P. E. *Langmuir* **1998**, *14*, 6130−6139.
(38) Fischer, D.; Curioni, A.; Andreoni, W. *Langmuir* **2003**, *19*, 3567−3571.
(39) Kerdcharoen, T.; Birkenheuer, U.; Krüger, S.; Woiterski, A.; Rösch, N. *Theor. Chem. Acc.* **2003**, *109*, 285−297.
(40) Franzen, S. *Chem. Phys. Lett.* **2003**, *381*, 315−321.
(41) Parr, R. G.; Yang, W. *Density-Functional Theory of Atoms and Molecules*; Oxford University Press: Oxford, 1989.
(42) Perdew, J. P.; Burke, K.; Ernzerhof, M. *Phys. Rev. Lett.* **1996**, *77*, 3865−3868; **1997**, *78*, 1396−1396.
(43) Hutter, J. et al. *CPMD V3.5*; Copyright IBM Corp 1990−2001, Copyright MPI für Festkörperforschung Stuttgart 1997−2001; see www.cpmd.org. Marx, D.; Hutter, J. In *Modern Methods and Algorithms of Quantum Chemistry*; Grotendorst, J., Ed.; NIC: FZ Jülich, 2000; pp 301−449; see www.theochem.rub.de/go/cprev.html.
(44) *CASTEP 4.2*, Academic version, licensed under the UKCP-MSI Agreement, 1999. Payne, M. C.; Teter, M. P.; Allan, D. C.; Arias, T. A.; Joannopoulos, J. D. *Rev. Mod. Phys.* **1992**, *64*, 1045−1097.
(45) Martyna, G. J.; Tuckerman, M. E. *J. Chem. Phys.* **1999**, *110*, 2810−2821.
(46) Vanderbilt, D. *Phys. Rev. B* **1990**, *41*, 7892−7895.
(47) The publicly available code by the Vanderbilt group was used; see www.physics.rutgers.edu/~dhv/uspp/.
(48) Frisch, M. J. et al. *GAUSSIAN98*; Gaussian Inc.: Pittsburgh, PA, 1998.

3. Results and Discussion

3.1. Structural Considerations. The obtained structures for M_n−ethylthiolate for M = Cu and Au are depicted in Figure 1. For the case of Cu, all species except the $n = 1$ cluster provide a 2-fold coordinated thiolate with Cu−S distances ranging in length from 2.19 to 2.25 Å with the longest bonds occurring for the $n = 9$ species. Similarly, Au_n−ethylthiolate species also show a relative uniformity of bond lengths across the series: Au−S bonds ranging from 2.35 to 2.39 Å for 2-fold coordinated sulfur (for the larger clusters $n > 3$) and 2.23 Å for singly coordinated S (for $n = 1$ and 3). Throughout all adducts, the S−C bond length ranges from 1.84 to 1.87 Å.

In comparison to the limiting behavior of a bulk metal surface as reference, it is noted that neither Cu nor Au clusters exhibit the same binding geometries. For the Cu(111) surface the thiolate is found to be 3-fold coordinated with Cu−S interactions consisting of two bond distances of 2.26−2.29 Å and a third one at 2.75 Å associated with a tilting of the 1.85 Å long S−C bond away from the surface normal. For the case of Au(111), 2-fold coordination is indeed obtained but with substantially longer Au−S distances of 2.46 Å and a shorter S−C bond of 1.83 Å; these numbers are in good agreement with calculated values reported in ref 21. The fact that the cluster structures do differ from that found on the surface suggests a priori that neither series of clusters will yield fragmentation energies entirely consistent with the bulk metal surface even for the largest values of n considered in this work.

3.2. Methylthiolates on Copper: Dissociation Channels. The goal of this section is to provide us with a *qualitative* understanding of the relative energetics of the various bonding motifs prevalent in the Cu_n−thiolate system and their dependence upon cluster size. To achieve these aims, we consider fragmentations of CH_3−$(CH_2)_m$−S−Cu_n adducts into the following products:

$$(CH_3{-}(CH_2)_m{-}S)^- + Cu_n^+ \quad (1)$$

$$CH_3{-}(CH_2)_m{-}S + Cu_n \quad (2)$$

$$(CH_3{-}(CH_2)_m{-}S)^+ + Cu_n^- \quad (3)$$

$$(CH_3{-}(CH_2)_m)^- + (Cu_n{-}S)^+ \quad (4)$$

$$CH_3{-}(CH_2)_m + Cu_n{-}S \quad (5)$$

$$(CH_3{-}(CH_2)_m)^+ + (Cu_n{-}S)^- \quad (6)$$

$$CH_3{-}(CH_2)_m{-}S{-}Cu_{n-2} + Cu_2 \quad (7)$$

$$CH_3{-}(CH_2)_m{-}S{-}Cu_{n-4} + Cu_4 \quad (8)$$

as a function of cluster size in the range $n = 1, 3, ..., 9$ and in this section only for the methyl systems, i.e., $m = 0$. Here, fragmentation pathways 1−3 describe scission of the Cu−S bond, pathways 4−6 correspond to breaking of the S−C bond, and pathways 7−8 describe cleavage of the metal cluster itself. The calculated fragmentation (i.e., dissociation or binding) energies $\Delta E = \sum E_{prod} - E_{adduct}$ are given in Table 1. For all of the fragmentation schemes, we take the two product fragments and optimize their structures separately to the respective nearest local minima. This leads in all cases, with the exception of $(Cu_5{-}S)^+$ (see below), to isostructural species. Thus, we have found that each fragment (with the above exception) adiabatically relaxed to a nearby isostructural minimum which is a likely occurrence if the process is thermally activated. On the other hand, it is unlikely to be valid if an external mechanical pulling force is applied to achieve fragmentation.[15] Pulling for instance with an AFM tip, while the cluster itself is fixed by one or several atoms to a surface,[15] might break the cluster and/or induce isomerization.[34] Thus, it should be stressed (see Introduction) that fragmentation under thermal activation and mechanical pulling may lead to very different fragmentation pathways.

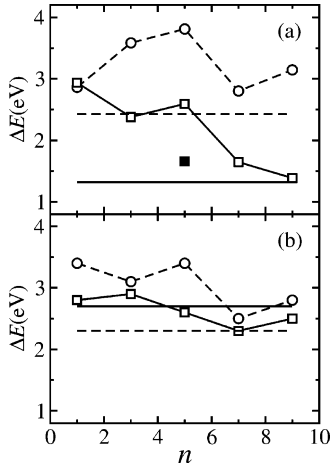

Figure 2. Fragmentation energies for breaking the S−C (squares and solid lines) and the M−S (circles and dashed lines) bonds for thiolates chemisorbed to M_n clusters. (a) Methylthiolate−Cu_n clusters and (b) ethylthiolate−Au_n clusters. The result for the three-dimensional Cu_5 isomer is shown by the filled square (see text). For reference, we also present corresponding energies obtained for Cu and Au(111) surfaces;[34] results for S−C and M−S bonds are marked by horizontal solid and dashed lines, respectively.

Table 1. Reaction Energies ΔE (eV) for Methylthiolate−Cu_n Adducts

no.	channel	$n = 1$	$n = 3$	$n = 5$	$n = 7$	$n = 9$
1	$(CH_3{-}S)^- + Cu_n^+$	9.5	7.9	8.6	7.2	6.9
2	$CH_3{-}S + Cu_n$	2.9	3.6	3.8	2.8	3.1
3	$(CH_3{-}S)^+ + Cu_n^-$	10.5	11.3	10.9	9.9	10.6
4	$(CH_3)^- + (Cu_n{-}S)^+$	11.7	8.3	8.8	7.9	6.9
5	$CH_3 + Cu_n{-}S$	2.9	2.4	2.6	1.6	1.4
6	$(CH_3)^+ + (Cu_n{-}S)^-$	10.8	10.1	9.9	9.3	9.0
7	$CH_3{-}S{-}Cu_{n-2} + Cu_2$		2.2	3.0	2.4	2.9
8	$CH_3{-}S{-}Cu_{n-4} + Cu_4$			3.3	3.5	3.4

The energy differences ΔE between the thiolated adducts and the dissociation products reported in Table 1 show that only two out of the eight pathways are energetically competitive, namely cleavage of the S−C bond, pathway 5, and fragmentation of the Cu cluster, pathway 7. In particular, *dissociation into neutral species* is always strongly energetically favored over dissociation into charged fragments so that only neutral species will be considered in the following discussion.

The most important fragmentation energies are plotted in Figure 2(a) in order to display more clearly trends as a function of cluster size n. The results show systematic and pronounced lowering of the S−C bond fragmentation energy (squares) with increasing cluster size. For the larger clusters, $n = 7$ and 9, this energy is close to the value of 1.3 eV as obtained for methylthiolate on a Cu(111) surface[34] using the same electronic structure method. Overall, the binding energy is found to decrease by more than a factor of 2 with respect to the limiting

Table 2. Reaction Energies ΔE (eV) for Ethylthiolate−Cu_n Adducts

no.	channel	$n=1$	$n=3$	$n=5$	$n=7$	$n=9$
2	$CH_3-CH_2-S + Cu_n$	2.8	3.6	3.9	2.9	3.2
5	$CH_3-CH_2 + Cu_n-S$	2.8	2.3	2.6	1.6	1.4
7	$CH_3-CH_2-S-Cu_{n-2} + Cu_2$		2.2	3.1	2.4	2.9
8	$CH_3-CH_2-S-Cu_{n-4} + Cu_4$			3.4	3.6	3.4
9	$CH_2=CH_2 + HS-Cu_n$			1.1		1.0

Table 3. Reaction Energies ΔE (eV) for Ethylthiolate−Au_n Adducts[a]

no.	channel	$n=1$	$n=3$	$n=5$	$n=7$	$n=9$
2	$CH_3-CH_2-S + Au_n$	3.4	3.1	3.4	2.5	2.8 (4.0)
5	$CH_3-CH_2 + Au_n-S$	2.8	2.9	2.6	2.3	2.5 (0.4)
7	$CH_3-CH_2-S-Au_{n-2} + Au_2$		1.9	3.1	0.8	2.7
8	$CH_3-CH_2-S-Au_{n-4} + Au_4$			3.3	2.3	1.9
9	$CH_2=CH_2 + HS-Au_n$		0.9	0.9	1.0	1.0

[a] Results for nonrelativistic reference calculations are given in parentheses.

case $n = 1$. Correspondingly, the S−C bond in the thiolate adduct is significantly destabilized in larger clusters.

The only exception from the trend seems to be the $n = 5$ case which needs some clarification. Bare Cu_5^-, Cu_5, and Cu_5^+ clusters are known to have planar shapes.[35] However, there exists also a three-dimensional (3D) Cu_5 isomer and its associated adduct and thus fragments, which is however ∼0.8 eV higher in energy compared to the 2D adduct. As mentioned above, the 3D cluster structure is important for the $(Cu_5-S)^+$ fragment. The relaxation of the higher energy 2D fragment to the 3D nonisostructural isomer is a result of the high electronic gradients observed in the initial structure as well as the relatively close energetics of 2D and 3D Cu_5 clusters. Hence, it is worthwhile to consider both isomers in order to test also the effect of cluster dimensionality upon the results. Calculation of fragmentation path 5 with the 3D Cu_5 constituent leads to a lowering of the S−C bond rupture to 1.7 eV; see the filled square in Figure 2a. Thus we observe a monotonic decrease of the S−C bond energy provided that Cu_n clusters of maximum dimensionality (for given n) are considered. We note in passing that effects of cluster dimensionality on adsorbate bond strengths have been observed previously for Au_n^+−methanol species where this phenomenon was employed as an experimental sensor to determine the cluster shape as probed by vibrational spectroscopy.[29,30]

A weak S−C bond for large n is consistent with experimental surface studies[7−11] which show desorption of hydrocarbon chains starting at temperatures of a few hundred Kelvin and full desorption at around 500 K. On the other hand, no systematic trend can be found for the Cu−S bond based on studying clusters as a function of n within the given size range. The (111) surface reference of about 2.4 eV, on the other hand, is consistently lower by about 0.5−1.4 eV and reflects the fact that binding to the cluster is different from that on the surface. Likewise, fragmentation energies of the metal subsystems are highly sensitive to the cluster structure for these small species as evidenced by the wide variation as a function of n for the energy of reaction 7 which oscillates on the order of 0.5 eV. These observations emphasize the differences in the chemistry of such small metal clusters as compared to bulk metal surfaces. For these species, the detailed energetics is still governed by the details of the cluster size and structure. Hence, it is surprising in this light that specifically the S−C binding energy has such a clear dependence on n and argues toward a mechanism that is only grossly dependent upon the cluster geometry but not on the thiolate binding configuration.

3.3. Role of Longer Chains: Ethylthiolates on Copper. We now turn to examine possible effects due to using longer chain thiolates. The calculated fragmentation energies involving ethylthiolates ($m = 1$) are collected in Table 2. First, we note that the fragmentation energies, also those of the high energy channels (see SI), are within 0.1 eV with those obtained for the methylthiolate cases (Table 1). This supports earlier observations that increase of the chain length has only a small effect on the metal−thiolate binding.[23,40]

Second and more importantly, in addition to evaluating the magnitude of the effect of increasing carbon chain length on the various fragmentation channels, we also investigate an alternate fragmentation pathway not available to methylthiolates. In addition to the previous eight fragmentation channels, we consider a new reaction:

$$CH_3-(CH_2)-S-Cu_n \rightarrow H_2C=CH_2 + Cu_n-SH \quad (9)$$

which is the desorption of an unsaturated hydrocarbon molecule, i.e., carbon−carbon double bond formation upon fragmentation. Indeed, it turns out to be the preferred channel for medium sized clusters, $n = 5$, and it is still competitive with S−C bond rupture at $n = 9$.

Evidence for the thermal desorption of unsaturated hydrocarbons, among a variety of other species, has been indeed reported on bulk surfaces.[11] In light of the presence of a third viable low energy fragmentation path, reaction 9, it is important to consider the role that the reaction path might play in determining which products may be observed. Calculations employing the standard QST2 reaction path algorithm[48] find that both reactions 2 and 5 for $n = 5$ occur without a barrier; i.e., the energy smoothly goes uphill as the two product species are separated. However, attempts to find a simple reaction path where the first step was hydrogen transfer to Cu metal via a β-agostic[50] type interaction for the lowest energy reaction 9 for $n = 5$ were unsuccessful. Other attempts to locate a simple path between the products and reactants also were inconclusive. This suggests that a more complex multistep process, possibly via first undergoing the barrierless reaction 5 and then subsequently transferring hydrogen back to the cluster, seems the most plausible. Such a multistep process *may* not be kinetically the most favorable one under the conditions of either thermal desorption experiments or an external pulling force as exerted by an AFM. Therefore, although reaction channel 9 yields a thermodynamically favorable dissociation state, the degree to which it may be observed is expected to largely depend on the specific conditions of the experiment.

3.4. Comparison with Gold. Fragmentation into charged species for thiolate−Au_n adducts has been addressed in detail elsewhere[23] where it was also found that these channels are significantly higher in energy and hence will not be considered here. Fragmentation energies into neutral products are summarized in Table 3 and Figure 2b for the $n = 1$, 3, 5, 7, and 9

(49) Flükiger, P.; Lüthi, H. P.; Portmann, S.; Weber, J. *MOLEKEL 4.0*; Swiss Center for Scientific Computing: Manno, Switzerland, 2000.
(50) Labinger, J. A.; Bercaw, J. E. *Nature* **2002**, *417*, 507−514.

Au_n species. It is noted that calculations employing multiple different thiolate binding sites on the largest cluster invariably lead to similar binding geometries and fragmentation energies within 0.2 eV of those reported here. Hence, we are confident that the observed trends reflect more the properties of the cluster than the details of how the thiolate is bound to it. In all the obtained species, with the exception of the $n = 3$ cluster, the thiolate prefers a 2-fold coordination pattern similar to that reported on the Au(111) surface.[18−21]

Similarly, as in the case of thiolate−Cu_n clusters, the lowest energy channel is found to be fragmentation into ethylene and a Au_n−SH cluster at all sizes with an exception of $n = 7$. Here too, it is expected that this reaction proceeds by a complex multistep mechanism and may not necessarily be observed depending on the experimental conditions. The next lowest energy channel is fragmentation of the cluster core into a smaller Au_k ($k < n$) cluster and a Au_{n-k}−thiolate adduct, the only exception being 2D $n = 5$ species where it is 0.5 eV higher in energy than S−C bond rupture. For the smallest Au_n clusters studied (≤ 5), cleavage of the S−C bond is found to be about the same as that observed on Cu_n clusters. However, unlike the scenario for copper, increasing the cluster size has only a marginal effect on weakening this bond. Specifically, the S−C bond energy decreases by only about 10% as the cluster size is increased from $n = 3$ to $n = 9$ as opposed to about 50% found for thiolate on Cu_n clusters. As a result the S−C bond cleavage energy in the thiolate bound to Au_9 is 1.1 eV higher than that of the copper analogue. Unlike copper, desorption of the thiolate molecule decreases in energy from $n = 3$ to $n = 9$ such that it also becomes competitive with S−C bond rupture for the larger species. To check that these findings do not arise from our assumption of employing cluster geometries structurally analogous to those of copper, we repeat the calculations using a previously studied low energy Au_9 species.[29] The cluster is only 0.1 eV lower in energy than the isomer isostructural to the copper one and yields reaction energies for thiolate desorption and S−C bond rupture of 3.3 eV and 2.7 eV, respectively. This confirms that the observed trends are preserved even when employing a quite different cluster geometry.

As with copper we compare these results with an estimate based on the binding energies obtained on a gold surface. The estimate 2.3 eV for the binding energy of the thiolate radical from the surface is larger than the experimental value of 1.7 ± 0.2 eV quoted in ref 12 but 0.5 eV less than obtained for the $n = 9$ cluster. The estimate for the rupture of the S−C bond is found to be about 2.7 eV, i.e., slightly larger than that for M−S rupture, indicating that the value for S−C bond rupture is closer to the value obtained for the smaller clusters and that for species larger than $n = 9$ one would expect this energy to again increase. Most notably, the surface result is qualitatively different from the cluster results since in the latter case scission of the S−C bond is preferred over *M*−S rupture at all cluster sizes. Overall, the thiolate−gold surface interaction is not as well represented by the small clusters as is its copper analogue but does retain the feature that the pronounced weakening of the S−C bond is lacking.

To conclude this section, we stress that although the reaction energies of various fragmentation paths are closely related to the thermally induced bond breaking events, they cannot automatically be used to asses fragmentation paths realized in possible mechanochemistry experiments (see Introduction). The result of mechanical pulling a thiolate chain from a Cu cluster or surface essentially depends also on energy barriers and gradients exerted along the reaction coordinate.[15,17]

3.5. Nonrelativistic Gold. Relativistic effects (RE) have long been recognized to be crucial in understanding the chemistry of gold.[24,26] Given otherwise formally equivalent occupations of outer electronic shells, our observations of bonding differences between Cu− and Au−thiolates can therefore be attributed, in general terms, to such effects. However, we stress that it is difficult to predict a priori the effect of relativity *on a particular property* such as the ratio of bond strengths involving the metal−thiolate junction, i.e., the M−S and S−C bonds. This is underscored by the finding in ref 19 where it was observed that (artificially) switching off relativity leads to strengthening of the Au−S bonds on a Au(111) surface, whereas the *opposite* is true for thiolate bound to just a single Au atom. This study,[19] however, does not address how this may influence the S−C bond strength, a crucial issue which is among the primary topics of this study. To this end, it is clearly mandatory to examine the hypothetical situation where RE are neglected for gold. To achieve this, we have constructed a nonrelativistic (NR) norm-conserving pseudopotential.[51] Based on tests (see SI), we are confident that this prescription will allow us to reliably capture the essence of bonding in hypothetical NR ethylthiolate−Au_n adducts.

We now consider fragmentation energies for an NR thiolate−Au_9 adduct. In qualitative agreement with ref 19, our model also finds that the weaker binding of thiolate to Au, relative to Cu, is a result of RE, resulting into dramatic changes in both structure and energetics of the adduct. The Au−S interaction retains its 2-fold bonding structure; however, the bond length increases from 2.36 to 2.94 Å in the NR limit, which is accompanied by an expansion of the Au_9 cluster core as expected. Despite this pronounced lengthening of the Au−S bond, we observe a significant increase in the thiolate binding energy, from 2.8 eV to 4.0 eV in the NR case. Even more notable is the observation that dissociation into Au_9S and C_2H_5 is dramatically lowered from 2.5 eV to 0.4 eV. Thus, for the NR gold cluster, the trend is to strengthen the metal−sulfur bond and, simultaneously, to lower the S−C binding energy signaling a strong preference of S−C bond scission over Au−S rupture as induced by the neglect of RE. This trend is remarkable also when comparing copper and relativistic gold; see Tables 2 and 3. In a nutshell, one could say that the neglect of RE in Au adducts leads to a behavior that mimics that of Cu adducts. Hence, it is directly verified that the essential difference between the stability of the metal−molecule junction of thiolates bound to copper and gold, in particular the *relative* strength of the S−C bonds, is largely due to relativistic effects on the electronic structure.

3.6. Bonding in Thiolated Copper and Gold Clusters. To provide an understanding of the chemical bonding with a clear focus on the difference between copper and gold, it is useful to consider first a simple qualitative descriptor. Given that copper is less electronegative than sulfur, one would be tempted to formally assign the S atom with a negative charge and the Cu cluster with a positive charge. This conceptual procedure would

(51) Hartwigsen, C.; Goedecker, S.; Hutter, J. *Phys. Rev. B* **1998**, *58*, 3641−3662.

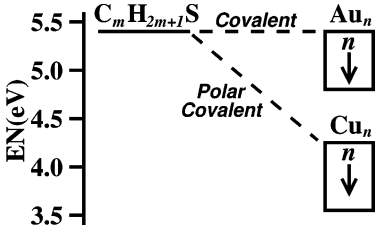

Figure 3. Schematic representation of trends in ENs between thiolate radicals, Au_n and Cu_n ($n \geq 5$) and its effect upon metal−sulfur bonding. The scheme is based upon computed EN values defined as EN = (IP + EA)/2, where IP is ionization potential and EA electron affinity.

result in an ionic picture of thiolate−metal bonding along with the associated nondirectionality in the thiolate−copper interaction. As already mentioned above, this is strikingly distinct from the thiolate−Au SAMs where the current view is of a more covalent and directional Au−S interaction. The Cu−S bonding in the methylthiolate−Cu(111) system was studied in ref 19 in detail. Based on the Mulliken population analysis, the authors have concluded that the thiolate−copper interaction is strongly covalent, while thiolate−gold interaction acquires some covalent features after inclusion of relativistic effects. However, advocating a strongly covalent thiolate−Cu bond compared to the thiolate−Au analogue appears counterintuitive if relativistic effects are responsible for covalent character of the bonding. A similar conclusion is obtained when one considers the electronegativity (EN) argument given above and the fact that Au is more electronegative than Cu.

Consider the calculated ENs of relevant fragments which can help to distinguish between covalent and ionic bonds; see Figure 3 for a schematic representation. The calculated EN value, obtained by the Mulliken definition, is found to be 5.4 eV for both methyl- and ethylthiolate radicals in agreement with the data given in ref 41 (see Table F.3 therein). This results from the fact that both HOMO and LUMO orbitals involved in ionization and electron capture are predominantly centered on the S atom. The EN values of $n \geq 5$ Au_n clusters are found to range between 4.7 and 5.4 eV with the larger clusters having a propensity toward a small EN value due to a lower ionization potential. This results in a small EN difference between Au_n clusters and thiolate, leading to a rather covalent and thus directional Au−S interaction, which supports alternate earlier assessments.[21,23,52,53] In comparison, $n \geq 5$ Cu_n clusters are found to have much smaller EN values ranging between 3.6 and 4.2 eV, again with a propensity toward lower EN values for larger clusters which compares well with theoretical and experimental data as reported in Table 6 of ref 36. Hence, the Cu_n and thiolate radicals have a larger EN difference ranging from 1.2 to 1.8 eV and thus should have a more ionic or polar covalent bonding interaction than their Au_n counterparts. Note that this interpretation fits *qualitatively* well with our observations above that NR Au behaves more like Cu in that absence of relativity decreases IP and EA of Au. Hence, NR Au clusters lower their EN and thus lead to a more ionic nature of Au−S bonding akin to copper.

The effect of an increased ionicity in the M−S interaction upon the S−C bond strength can be understood in a simple way. To illustrate, consider the hypothetical fragmentation on

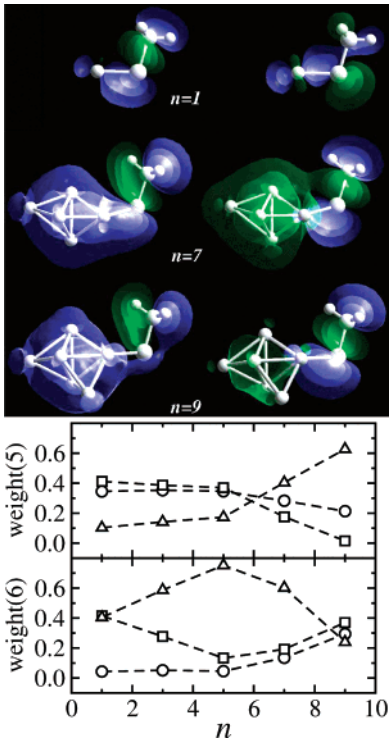

Figure 4. Analysis of S−C bond weakening in CH_3−S−Cu_n. (Upper panel) Spatial distribution of Kohn−Sham eigenstates # 5 (left column) and # 6 (right column) for $n = 1$, 7, and 9. Blue/green color indicates the sign of the wavefunction. (Lower panel) Corresponding Mulliken population analysis for the orbitals #5 (upper subpanel) and #6 (lower subpanel) as a function of cluster size; results for p orbitals on C (circles) and S (squares) are summations over p_x, p_y, and p_z projectors, and results for Cu (triangles) are sums over 4s and 3d projectors

X−S−C_2H_5 (X = H, Li, and Na) into X−S and C_2H_5 radicals. For these isostructural molecules, one can view this by the simplified idea that the H−S interaction represents a covalent interaction, whereas the Na−S represents a more ionic scenario and Li−S is an intermediate case. The S−C bond in the ethylthiol molecules is estimated to fragment into H−S and C_2H_5 with an energy of about 3.3 eV as estimated with the PBE/TZVP approach. By replacing H by Li or Na, the sulfur atom becomes negatively charged and polarizes the S−C bond to give a calculated fragmentation energy of 3.1 eV and 2.9 eV, respectively. Extending this *qualitative* reasoning to the case of Cu_n clusters, a polar covalent Cu−S bond leaves a stronger net negative charge upon the sulfur atom which in turn weakens the S−C bond making the Cu_nS + alkylradical fragmentation channel more favorable at larger *n*. However, the trend is by no means quantitative in that it neglects the actual charge distribution within the cluster itself as well as orbital effects such as ligand−metal back-donation of electronic charge. Finally, a similar electrostatic mechanism, although much less pronounced, has already been advanced to explain the weakening of the C−O bond observed on charged methanol−Au_n^+ clusters,[29,30] and it appears that a similar mechanism is in operation here for thiolate−Cu interaction.

As a complementary assessment, we consider a more detailed electronic structure analysis using the one-electron orbital picture. The main features governing the S−C bond weakening as a function of the metal cluster size can be gleaned from the spatial distribution of just a few eigenstates; see Figure 4. The other tool used to obtain a more detailed information on

(52) Andreoni, W.; Curioni, A.; Grönbeck, H. *Int. J. Quantum Chem.* **2000**, *80*, 598−608.
(53) Basch, H.; Ratner, M. A. *J. Chem. Phys.* **2003**, *119*, 11926−11942.

electronic structure is the Mulliken population analysis (MPA) by projecting Kohn−Sham molecular orbitals (MOs) expanded in plane-waves onto a minimal basis set composed of numerical (pseudo)valence atomic orbitals of S, C, H, and Cu atoms.[54] Taking into account the well-known drawbacks and caveats of MPA itself and the intermediate projection step, this analysis allows us to identify the most significant *relative trends* if studied as a function of cluster size. The spilling parameter, indicating the quality of the projection of eigenstates onto the localized orbitals, is always around 1%, indicating almost complete projection onto the minimal basis set.

The findings from MPA and wave function analysis in Figure 4 can be summarized as follows. The two lowest eigenstates at ~ -18.5 eV and ~ -15 eV correspond to bonding and antibonding C(2s)−S(3s) σ-type MOs, respectively. These MOs change only slightly upon variation of the number of Cu atoms in the cluster. The MOs #3 and #4 are mainly S−C π-type bonding orbitals formed largely by C($2p_x$), C($2p_y$) and by S($3p_x$), S($3p_y$) AOs. The lower one of these orbitals loses a part of its S−C population with increasing cluster size (about 10% of the charge moves toward the Cu−S region), which, though, weakens the S−C bond only slightly. Of all eigenstates there are just two which are significantly populated by C(2p) and/or S(3p) electrons *and* simultaneously exhibit a strong dependence on the size of the Cu cluster. These are MOs #5 and #6, both composed of C($2p_z$), S($3p_z$), and Cu(3d) contributions, which have energies around −9 eV and change in separation energy by 2 eV to 0.5 eV. These MOs are positioned below the bottom of the Cu(3d) and Cu(4s) range of energies, and for large clusters they are similar to "impurity levels" in the Cu(3d) "band" which is in the range ~ -8 eV to ~ -4 eV. For $n = 1$, the lower orbital is strongly populated on the S−C bond (forming a σ-type bonding orbital), and the higher one (which has a more complicated spatial distribution and less bonding character) gives very little population into the S−C bond. Increasing the cluster size causes (apart from the creation of two quasi-symmetrical Cu−S contacts) the S−C bonding contribution in MO #5 to decrease. This is counterbalanced by a simultaneous gain of population in MO #6; see Figure 4. Close examination of Figure 4 also shows that actually a crossover occurs around $n = 5$ in concurrence with the enhancement of the weakening of the S−C bond upon the 2D−3D cluster structural transition. In agreement with our simple model based on electrostatics, the increase in the interaction with the larger Cu cluster results in a mixing of *occupied* S−C MOs on the thiolate, such that the S($3p_z$) population is transferred from MO #5 to the higher in energy MO #6, thus weakening the S−C bond.

4. Summary and Conclusions

We have performed a first principles electronic structure study of possible fragmentation scenarios of metal−thiolate junctions based on small coinage metal clusters. In particular, adducts of the form $CH_3-(CH_2)_m-S-M_n$ (using M = Cu, Au; $m = 0, 1$; $n = 1, 3, 5, 7, 9$) were investigated in order to analyze rupture channels but in particular chemical bonding as a function of cluster size. In the limit of small ($n < 5$) clusters, the energetically most favorable reaction channels investigated are desorption of *unsaturated* hydrocarbons and metal cluster fragmentation for both Cu and Au. However, in particular the formation of C=C double bonds seems to be a complex process so that details of the experimental conditions are expected to be crucial in favoring a particular channel.

Our most significant finding is to uncover a pronounced and systematic *weakening* of the S−C bond, by over 1 eV in energy, upon increasing the size of the Cu_n cluster beyond $n = 5$. This effect is clearly not observed for gold but matches well with the experimental observation of the thermal desorption of hydrocarbons from SAMs on bulk Cu surfaces. This observation of a dramatic decrease in the energy required to rupture the S−C bond of a thiolate chemisorbed on a Cu_n cluster and its n dependence can be explained by invoking an electrostatic mechanism, namely polarization of the S−C bond induced by the polar bonding of thiolate to Cu_n. Although M−S binding is stronger in Cu than in Au, the above evidence points rather to the fact that the Au−S interaction is more covalent than its Cu analogue. On the other hand, for Au, relativistic contributions to the bonding lead to a weaker and more covalent metal−thiolate interaction where S−C bond weakening is mitigated. In a nutshell, hypothetical nonrelativistic gold behaves similar to copper with an even more pronounced propensity for S−C bond rupture. Overall, in the limit of large n, as ultimately represented by bulk metal surfaces, S−C bond fragmentation is energetically much more favorable to thiolate desorption for copper, which is not true for gold.

Some interesting ramifications of our findings are that thiolate species on both Cu nanoparticles and surfaces are highly likely to undergo thermal degradation resulting in desulfurization of the organic molecule, to sulfide formation and thus to poisoning of copper. This observation, among other disadvantages, calls into question the usefulness of thiolate−copper nanojunctions, but it would be interesting to see if this effect could be lessened somewhat when using a solvent with a high dielectric constant.[55] In addition, quite different scenarios might be expected for the very same reason when using Cu instead of Au in AFM-type or mechanical-controllable break-junction experiments involving thiolate-functionalized molecules. Of more academic interest is the modulation of the S−C bond weakening by the 2D to 3D cluster structural transition. Confirmation of our findings could be accomplished by exploiting the above observation to employ thiolates as a chemical sensor to *experimentally* distinguish the 2D to 3D structural transition in neutral Cu_n clusters in an analogous way as observed for methanol on Au_n^+ species.[29,30]

Acknowledgment. We are indebted to B. Meyer for providing us with ultrasoft pseudopotentials and to Ch. Wöll for stimulating discussions. This work was partially supported by Volkswagen-Stiftung under the project STRESSMOL and by FCI. M.K. and I.Š. acknowledge financial support by the Slovak APVT agency under the project number APVT-20-019202. Computer resources were provided by Scientific Supercomputing Center Karlsruhe SSCK, BOVILAB@RUB, and CCMS.

Supporting Information Available: Benchmark calculations compared to available experimental data, results comparisons

(54) Sanchez-Portal, D.; Artacho, E.; Soler, J. M. *Solid State Commun.* **1995**, *95*, 685−690.

(55) Ron, H.; Cohen, H.; Matlis, S.; Rappaport, M.; Rubinstein, I. *J. Phys. Chem. B* **1998**, *102*, 9861−9869.

from plane-waves vs Gaussian basis sets, 19-electron Cu pseudopotential tests, DFT and MP2 results, detailed data for the longer chain length species, the NR gold pseudopotential tests, and details of the surface calculations. This material is available free of charge via the Internet at http://pubs.acs.org.

JA047946J